Gravitational waves from the remnants of the first stars

Mon. Not. R. Astron. Soc. **000**, 1–6 (2016) Printed 20 September 2018 (MN LATEX style file v2.2)

Gravitational waves from the remnants of the first stars

Tilman Hartwig[1⋆], Marta Volonteri[1], Volker Bromm[2], Ralf S. Klessen[3], Enrico Barausse[1], Mattis Magg[3], and Athena Stacy[4]

[1] *Sorbonne Universités, UPMC et CNRS, UMR 7095, Institut d'Astrophysique de Paris, 98 bis bd Arago, F-75014 Paris, France*
[2] *Department of Astronomy, University of Texas, Austin, Texas 78712, USA*
[3] *Universität Heidelberg, Zentrum für Astronomie, Institut für Theoretische Astrophysik, Albert-Ueberle-Str. 2, D-69120 Heidelberg, Germany*
[4] *Department of Astronomy, University of California, Berkeley, CA 94720, USA*

20 September 2018

ABSTRACT

Gravitational waves (GWs) provide a revolutionary tool to investigate yet unobserved astrophysical objects. Especially the first stars, which are believed to be more massive than present-day stars, might be indirectly observable via the merger of their compact remnants. We develop a self-consistent, cosmologically representative, semi-analytical model to simulate the formation of the first stars. By extrapolating binary stellar-evolution models at 10 % solar metallicity to metal-free stars, we track the individual systems until the coalescence of the compact remnants. We estimate the contribution of primordial stars to the merger rate density and to the detection rate of the Advanced Laser Interferometer Gravitational-Wave Observatory (aLIGO). Owing to their higher masses, the remnants of primordial stars produce strong GW signals, even if their contribution in number is relatively small. We find a probability of $\gtrsim 1\%$ that the current detection GW150914 is of primordial origin. We estimate that aLIGO will detect roughly 1 primordial BH-BH merger per year for the final design sensitivity, although this rate depends sensitively on the primordial initial mass function (IMF). Turning this around, the detection of black hole mergers with a total binary mass of $\sim 300\,\mathrm{M}_\odot$ would enable us to constrain the primordial IMF.

Key words: black hole physics – gravitational waves – stars: Pop III – early Universe

1 INTRODUCTION

The first detection of gravitational waves (GWs) on 2015 September 14, has opened a completely new window to investigate astrophysical processes and phenomena, which are otherwise invisible to observations in the electromagnetic spectrum (but see Loeb 2016; Perna et al. 2016). This first event GW150914 was the inspiral and merger of two black holes (BHs) with masses $M_1 = 36^{+5}_{-4}\,\mathrm{M}_\odot$ and $M_2 = 29^{+4}_{-4}\,\mathrm{M}_\odot$ at redshift $z = 0.09^{+0.03}_{-0.04}$ (Abbott et al. 2016b). It was detected by the Advanced Laser Interferometer Gravitational-Wave Observatory (aLIGO) with a false alert probability of $< 2 \times 10^{-7}$ (Abbott et al. 2016b). The local merger rate density inferred from this event is $2 - 400\,\mathrm{yr}^{-1}\mathrm{Gpc}^{-3}$ for BH–BH mergers (Abbott et al. 2016c). GW150914 also indicates that the stochastic GW background could be higher than previously expected and potentially measurable by the aLIGO/Virgo detectors operating at their final sensitivity (Schneider et al. 2000; Abbott et al. 2016a).

The detection probability increases with the mass of the merging BHs. The first, so-called Population III (Pop III), stars are believed to be more massive than present-day stars and yield consequently more massive remnants (for reviews see Bromm 2013; Glover 2013; Greif 2015). Due to their high masses, a significant fraction of the possible detections might originate from these primordial stars (Belczynski et al. 2004; Kulczycki et al. 2006; Kinugawa et al. 2014, 2016) and Dominik et al. (2013, 2015) show that most of the binary BHs that merge at low redshift, have actually formed in the early Universe. Hence, it is worth investigating the contribution from Pop III stars in more detail with a self-consistent model of primordial star formation.

In this Letter, we apply a semi-analytical approach to determine the rate density and the detection rate of mergers for aLIGO that originate from the first stars.[1]

⋆ E-mail: hartwig@iap.fr

[1] Our catalogues of Pop III binaries are publicly available here: `http://www2.iap.fr/users/volonter/PopIIIGW`

2 METHODOLOGY

2.1 Self-consistent Pop III star formation

We create a cosmologically representative sample of dark matter merger trees with the GALFORM code based on Parkinson et al. (2008). The merger trees start at $z_{\rm max} = 50$ and follow Pop III star formation down to $z = 6$, after which we do not expect significant Pop III star formation to occur. The formation of primordial stars is modelled self-consistently, taking into account radiative and chemical feedback. We briefly review the main aspects of the model; see Hartwig et al. (2015a,b) for details.

To form Pop III stars, a halo has to be metal free and have a virial temperature high enough for efficient cooling by H_2. Moreover, we check the time-scale of dynamical heating due to previous mergers and the photodissociation of H_2 by external Lyman–Werner radiation. Once a dark matter halo passes these four criteria, we assign individual Pop III stars to it, based on random sampling of a logarithmically flat initial mass function (IMF) in the mass range between $M_{\rm min} = 3\,{\rm M}_\odot$ and $M_{\rm max} = 300\,{\rm M}_\odot$, motivated by, e.g., Greif et al. (2011), Clark et al. (2011), and Dopcke et al. (2013). The IMF is still uncertain, and therefore besides this fiducial model, we also consider a low mass ($1 - 100\,{\rm M}_\odot$) and a high mass ($10 - 1000\,{\rm M}_\odot$) IMF. The total stellar mass per Pop III-forming halo is set by the star formation efficiency. This parameter is calibrated to reproduce the optical depth to Thomson scattering of $\tau = 0.066 \pm 0.016$ (Planck Collaboration 2015), taking also into account the contribution by later generations of stars, based on the global cosmic star formation history (Behroozi & Silk 2015).

2.2 Binary sampling and evolution

We use the results of the most detailed study of Pop III binary systems to date by Stacy & Bromm (2013). They performed a cosmological simulation initialized at $z = 100$ within a 1.4 Mpc (comoving) box. This simulation followed the eventual formation and evolution of Pop III multiple systems within 10 different minihaloes at a resolution of 20 au. From this study, we adopt a binary fraction of 36%, which translates into a $\sim 50\%$ probability for a single star to have a binary companion (see also Stacy et al. 2016). Note that other studies of Pop III star formation might allow larger binary fractions (Clark et al. 2011; Greif et al. 2011; Smith et al. 2011), but all derived merger and detection rates scale linearly with this binary fraction. Our results can thus readily be rescaled accordingly.

The evolution of the binary system and consequently the nature (BH or NS), the masses, and the time of coalescence of the two compact objects depend mainly on the zero-age main-sequence (ZAMS) characteristics, respectively, the semimajor axis and eccentricity of their orbit and their masses. For the pairing of the binaries and the underlying distribution of mass ratios, we apply the 'ordered pairing' advocated by Oh et al. (2015), since observations show that massive binaries favour members with similar masses. Hence, we order the primordial stars in one halo by descending mass, check probabilistically if they have a binary companion, and pair the most massive with the second most massive, the third most massive with the fourth most massive and so on. For the ZAMS eccentricity e_0 of each binary system we draw a random value from the thermal distribution $p(e)\,{\rm d}e \propto e\,{\rm d}e$ with $e_{\rm min} = 0.1$ and $e_{\rm max} = 1$ (Kroupa 1995; Dominik et al. 2012; Kinugawa et al. 2014, hereafter K14). This distribution agrees qualitatively with that in Stacy & Bromm (2013). The ZAMS semimajor axis a_0 is sampled from the distribution $p(x)\,{\rm d}x \propto x^{-1/2}\,{\rm d}x$ with $x = \log(a_0/{\rm R}_\odot)$, $a_{\rm min} = 50\,{\rm R}_\odot$, and $a_{\rm max} = 2 \times 10^6\,{\rm R}_\odot$. The shape and the lower limit are motivated by Sana et al. (2012) and de Mink & Belczynski (2015) (hereafter dMB15), whereas the upper limit is chosen in agreement with the data by Stacy & Bromm (2013). We have verified that the specific choice of these limits does not significantly affect the final results.

Once we have identified the binaries and assigned their ZAMS quantities, we use the tabulated models for stellar binary evolution by dMB15 to calculate the masses of the remnants and their delay time $t_{\rm del}$ until coalescence. The delay time is the sum of the time from the ZAMS to the formation of the last compact object and the ensuing inspiral time, $t_{\rm insp}$. We chose their model 'N-m2 A.002' (with the lowest available metallicity of 10% solar), as the best fit to the properties of Pop III stars in terms of IMF, metallicity, and evolutionary channels (see also K14; Belczynski et al. (2016), hereafter B16)

Notice the differences between the stellar binary evolution of metal-free and metal-enriched systems, which might lead to systematic errors (K14; K16). In contrast to metal-enriched stars, Pop III stars lose only a small fraction of their mass due to stellar winds, which yields more massive remnants and closer binaries, since the binding energy is not carried away by the winds. Moreover, Pop III stars with a stellar mass of less than $\sim 50\,{\rm M}_\odot$ evolve as blue supergiants (not as red supergiants, like metal-enriched stars) and the resulting stable mass transfer makes the common envelope phase less likely.

The data is tabulated for stellar masses of the individual companions of up to $150\,{\rm M}_\odot$. For higher masses, we proceed in the following way. We ignore binaries with one star in the mass range $140\,{\rm M}_\odot \leqslant M_* \leqslant 260\,{\rm M}_\odot$, as we do not expect any compact remnants due to pair-instability supernova (PISN) explosions (Heger & Woosley 2002). For stars above $260\,{\rm M}_\odot$, we consider $t_{\rm del}$ characteristic of stars with $100\,{\rm M}_\odot \leqslant M_* \leqslant 140\,{\rm M}_\odot$, adopt the final BH masses of primordial stars from Heger & Woosley (2002), and correct the tabulated inspiral time according to (K14) $t_{\rm insp} \propto {m_1}^{-1}{m_2}^{-1}(m_1 + m_2)^{-1}$, where m_1 and m_2 are the masses of the binary compact objects. This approach is justified because the tabulated $t_{\rm del}$ show negligible dependence on stellar mass for massive stars.

2.3 Detectability

Based on the cosmologically representative, self-consistent sampling of Pop III stars and the corresponding $t_{\rm del}$ of each binary, we determine the intrinsic merger rate density R. This represents the number of compact binary mergers per unit source time and per comoving volume, and is also referred to as the rest-frame merger rate density. To estimate the aLIGO detection rate, we calculate the single-detector signal-to-noise ratio (SNR) ρ for each merger via (Maggiore

2007; Finn & Chernoff 1993; Cutler & Flanagan 1994),

$$\rho^2 = 4\int_0^\infty \frac{|h(f)|^2}{S_n(f)}\mathrm{d}f\,, \quad (1)$$

where $h(f)$ is the Fourier-domain (sky- and orientation-averaged) GW strain at the detector, and S_n is the noise power spectral density of a single aLIGO detector. We assume that an event is detectable if $\rho > 8$, as conventionally done in the LIGO literature (Abadie et al. 2010; Dominik et al. 2015; Belczynski et al. 2016; de Mink & Mandel 2016). (This translates to SNR larger than 12 for a three-detector network, e.g. the two aLIGOs and advanced Virgo.) For the current aLIGO detectors, we use the O1 noise power spectral density (Abbott et al. 2015), whereas to assess detectability when the detectors are in their final design configurations we use the zero-detuning, high-power configuration of Abbott et al. (2009). For $h(f)$, we use either inspiral-only, restricted post-Newtonian waveforms (computing the Fourier transform with the stationary phase approximation, see e.g. Maggiore 2007), or inspiral-merger-ringdown PhenomA (non-spinning) waveforms (Ajith et al. 2008, 2009). We employ the former for BH–NS, and NS–NS systems, with a cut-off at the frequency of the innermost stable circular orbit (ISCO; note that the ISCO frequency also corresponds approximately to the merger frequency of NS–NS systems). For BH–BH systems, particularly at high masses, the merger-ringdown contains considerable SNR, hence we use PhenomA waveforms. We then calculate the detection rate as (Haehnelt 1994)

$$\frac{dn}{dt} = 4\pi c\int_{\substack{\rho>8\\ z<z_{\max}}} \mathrm{d}z\mathrm{d}m_1\mathrm{d}m_2 \frac{\mathrm{d}^2R}{\mathrm{d}m_1\mathrm{d}m_2}\frac{\mathrm{d}t}{\mathrm{d}z}\left(\frac{d_L}{1+z}\right)^2, \quad (2)$$

where the luminosity distance d_L and the derivative of the look-back time with respect to z, $\mathrm{d}t/\mathrm{d}z$, are computed with a ΛCDM cosmology, and the integral is restricted to detectable events only ($\rho > 8$).

Finally, we characterize the stochastic GW background of our binary population by the energy density spectrum (see e.g. Phinney 2001; Rosado 2011; Abbott et al. 2016a):

$$\Omega_{\mathrm{GW}}(f) = \frac{f}{\rho_c c^2}\int_{z<z_{\max}} \mathrm{d}z\mathrm{d}m_1\mathrm{d}m_2 \frac{\mathrm{d}^2R}{\mathrm{d}m_1\mathrm{d}m_2}\frac{\mathrm{d}t}{\mathrm{d}z}\frac{\mathrm{d}E_s}{\mathrm{d}f_s}, \quad (3)$$

where ρ_c is the critical density, and $\mathrm{d}E_s/\mathrm{d}f_s \propto (f|h(f)|)^2$ is the spectral energy density of a binary, computed at the source-frame frequency $f_s = f(1+z)$ (f being the frequency at the detector). Our model's prediction for Ω_{GW} should be compared with the 1σ power-law integrated curves (Thrane & Romano 2013) in Abbott et al. (2016a) for the aLIGO/advanced Virgo network in the observing runs O1 (2015 to 16) and O5 (2020–2022), which represent the network's sensitivity to standard cross-correlation searches (Allen & Romano 1999) of power-law backgrounds.

3 RESULTS

In Fig. 1, we compare our star formation rate (SFR) to other models. Our self-consistent Pop III SFR, with a peak value of $\mathrm{SFR}_{\max} = 2\times10^{-4}\,\mathrm{M}_\odot\,\mathrm{yr}^{-1}\,\mathrm{Mpc}^{-3}$, is in compliance with Visbal et al. (2015), who show that it cannot exceed a few $\times10^{-4}$, without violating the constraints set by Planck Collaboration (2015). K14 assume an SFR with a peak value of

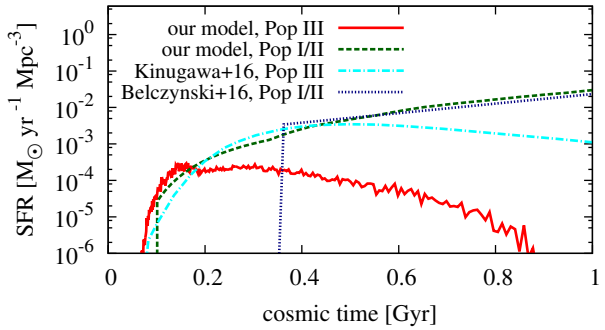

Figure 1. Comparison of our SFR for the fiducial IMF with the models used by Kinugawa et al. (2016) (hereafter K16) and B16. Our Pop I/II SFR, which is adopted from Behroozi & Silk (2015), is in good agreement with the corresponding SFR by B16. For the Pop III stars, our self-consistent modelling yields a peak SFR that is about an order of magnitude lower than the value by K16.

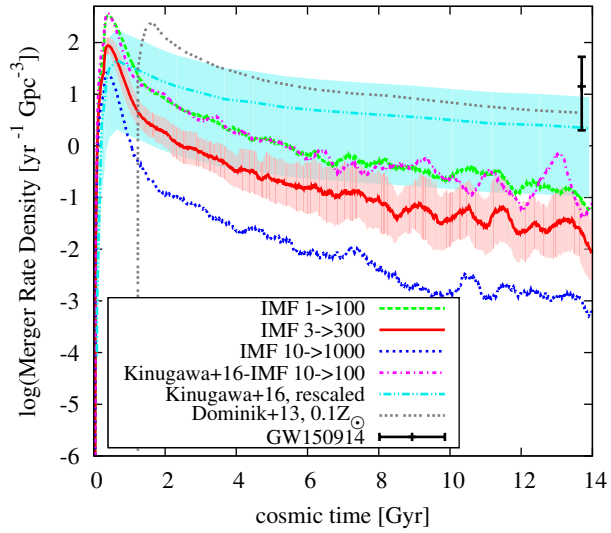

Figure 2. Intrinsic merger rate densities (BH–BH, BH–NS, and NS–NS) for our models and comparison to the literature. For clarity, we show the statistical variance as shaded region only for our fiducial model. We plot the model by K16 for Pop III remnants, (their fig. 22, model 'under100, optimistic core merger'), rescaled to our $\mathrm{SFR}_{\max}$ with the corresponding systematic uncertainty. The model by Dominik et al. (2013) determines the merger rate density for stars at 10% solar metallicity (their fig. 4). We also show the expected value at $z = 0$ from the GW150914 detection (Abbott et al. 2016c).

$\mathrm{SFR}_{\max} = 3\times10^{-3}\,\mathrm{M}_\odot\,\mathrm{yr}^{-1}\,\mathrm{Mpc}^{-3}$, which is about an order of magnitude higher than our result. The SFR is about the same for all our Pop III IMFs, because we calibrate each model to match τ. The exact redshift evolution of the Pop III SFR depends on the details of the treatment of reionization and metal enrichment (cf. Johnson et al. 2013, for a comparison).

The intrinsic merger rate density of compact objects can be seen in Fig. 2. To compare with K16 we rescale their SFR to our peak value, and run a case with their IMF (10–100). Our values are about an order of magnitude lower than the rescaled prediction by K16 in the regime relevant for GW

IMF	BH–BH	BH–NS	NS–NS	$m_1 > M_{\rm PI}$
1–100	5.3	1.4×10^{-2}	7.2×10^{-3}	0
3–300	0.48	2.1×10^{-3}	8.1×10^{-4}	0.011
10–1000	0.12	2.4×10^{-4}	1.1×10^{-5}	0.089

Table 1. Detection rates in events per year for aLIGO at final design sensitivity. Assuming a log normal distribution, we find a statistical scatter (1σ) between different independent realizations of $(0.04 - 0.43)$ dex, depending on the IMF and type of the merger. For the fiducial IMF (3–300), we expect about one Pop III binary BH every two years and for the lower mass IMF (1–100), even up to 5 detections per year. The probability to detect a merger that can uniquely be identified as being of primordial origin ($m_1 > M_{\rm PI}$) is highest for the high-mass IMF (10–1000) with about one detection per decade. Inversely, the strong dependence of the detection rate on the IMF can be used to infer the upper mass limit for Pop III stars.

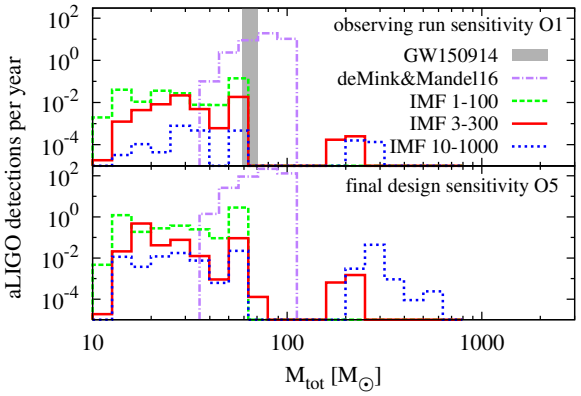

Figure 3. Expected number of BH–BH merger detections per year as a function of the total binary mass for the current aLIGO sensitivity (top) and final design sensitivity (bottom). The mass range of GW150914 is indicated by the grey area. With sufficient detections around $M_{\rm tot} \approx 300\,{\rm M}_\odot$, we could discriminate different Pop III IMFs based on their GW fingerprint.

detections, i.e. mergers occurring at late cosmic times. This is to be ascribed to the different binary evolution models. Given that K14 study explicitly Pop III star binary evolution, and we extrapolate models at higher metallicity, we conclude that our estimates are a lower limit to the GW detections of Pop III binaries by up to an order of magnitude. We stress, however, that our Pop III SFR is calculated self-consistently and reproduces the optical depth constraint set by Planck Collaboration (2015), in contrast to K14; K16.

Comparing models with different IMFs, the number of expected mergers is dominated by $M_{\rm max}$. This is because the remnants at low stellar masses are mostly NSs, which make only a small contribution to the overall merger rate. The merger rate density generally decreases with higher $M_{\rm max}$, because fewer stars (hence, binaries) form for a given total stellar mass. At face value, Pop III stars do not yield a major contribution to the total merger rate density, but we recall that our estimates are likely lower limits. Crucially, due to their higher masses, Pop III BH–BH mergers have strong GW signals, which boost their detection probability over lower mass BHs formed from later stellar generations.

Another essential question is whether we are able to discriminate mergers of primordial origin. The most massive remnant BHs for binaries at $0.1\,Z_\odot$ have a mass of $\sim 42\,{\rm M}_\odot$ (dMB15). All BHs with higher masses must be of primordial origin (though note that binary BHs with $M_{\rm tot}$ up to $\sim 160 M_\odot$ may form in globular clusters; Belczynski et al. 2014; Rodriguez et al. 2016). The minimal mass for Pop III remnant BHs above the PISN gap is $M_{\rm PI} \approx 200\,{\rm M}_\odot$. Since aLIGO will measure the source-frame total mass for $M_{\rm tot} \gtrsim M_{\rm PI}$ within a 20% uncertainty at the 2-σ level (Graff et al. 2015, see also Veitch et al. 2015; Haster et al. 2016), we can use $M_{\rm PI}$ as the threshold for the unambiguous detection of a primordial BH. For IMFs extending above $300\,{\rm M}_\odot$ about one BH–BH merger per decade can be unambiguously attributed to a Pop III binary (Table 1). As discussed above, this is plausibly a lower limit because of the too efficient mass loss and hence, the underestimated remnant masses in our binary evolution model.

To distinguish the contributions to the detection rate by different generations of stars (also below $M_{\rm PI}$) we show the specific detection rates as a function of $M_{\rm tot} = m_1 + m_2$ in Fig. 3. We compare our three different IMFs with a model by de Mink & Mandel (2016). They determine the detection rate of Pop I/II stars for the chemically homogeneous evolutionary channel for binary black hole mergers, which dominates at $30\,{\rm M}_\odot \lesssim M_{\rm tot} \lesssim 100\,{\rm M}_\odot$. For a given $M_{\rm tot}$ the histogram enables to determine the probability that this event has a primordial origin. For GW150914, this probability is $\gtrsim 1\%$ (see B16; Woosley 2016, for different approaches). For detections around $\sim 300\,{\rm M}_\odot$, in addition to unambiguously establishing a Pop III origin, one can even distinguish different Pop III IMFs by their number of detections over the next decades.

In our models, the highest stochastic GW background is produced by BH–BH mergers, and at $f \approx 25$ Hz (where the network is most sensitive), $\Omega_{\rm GW}(25\,{\rm Hz}) \approx 4 \times 10^{-12} - 1.4 \times 10^{-10}$ (the range corresponds to different IMF choices; the inclusion or removal of resolved sources only makes a negligible difference). For comparison, the stochastic background at 25 Hz inferred from GW150914 is $\Omega_{\rm GW}(25{\rm Hz}) = 1.1^{+2.7}_{-0.9} \times 10^{-9}$ at 90% confidence level, and the aLIGO/advanced Virgo network 1σ sensitivity (corresponding to SNR = 1) for two years of observation at design sensitivity (O5) is $\Omega_{\rm GW}(25{\rm Hz}) = 6.6 \times 10^{-10}$. The stochastic background produced by Pop III remnant mergers is therefore negligible at the relevant frequencies (compare Dvorkin et al. 2016, but see Inayoshi et al. 2016).

4 DISCUSSION

We have estimated the GW fingerprint of Pop III remnants on the aLIGO data stream. GWs have the potential to directly detect the remnants of the first stars, and possibly even to constrain the Pop III IMF by observing BH–BH mergers with a total mass around $M_{\rm tot} \approx 300\,{\rm M}_\odot$. The latter is the key to ascertain the impact of the first stars, due to their radiative and supernova feedback, on early cosmic evolution. The new GW window ideally complements other probes, such as high-z searches for energetic supernovae with the *James Webb Space Telescope (JWST)*, or stellar archaeological surveys of extremely metal-poor stars (Bromm 2013). We have developed a model which includes Pop III star formation self-consistently, anchored, within the uncertainties, to the Planck optical depth to Thomson scat-

tering. The main caveats in this study arise from the still uncertain Pop III binary properties and the corresponding stellar binary evolution.

We find a probability of $\gtrsim 1\%$ that GW150914 originates from Pop III stars, although this number may increase with improved future modelling. Crucially, the higher masses of the first stars boost their GW signal, and therefore their detection rate. Up to five detections per year with aLIGO at final design sensitivity originate from Pop III BH–BH mergers. Approximately once per decade, we should detect a BH–BH merger that can unambiguously be identified as a Pop III remnant. It is exciting that the imminent launch of the *JWST* nearly coincides with the first direct detection of GWs, thus providing us with two powerful, complementary windows into the early Universe.

GWs from BH binaries originating from Pop III stars may also be detectable by the *Einstein Telescope* (Sesana et al. 2009) or (in their early inspiral) by eLISA (Amaro-Seoane & Santamaría 2010; Sesana 2016), which would allow probing the physics of these systems with unprecedented accuracy.

Acknowledgements

We thank P. Kroupa, S. Glover, M. Latif, D. Whalen, S. Babak, C. Belczynski, and the referee for helpful contributions. We acknowledge funding under the European Community's Seventh Framework Programme (FP7/2007-2013) via the European Research Council Grants 'BLACK' under the project number 614199 (TH, MV) and 'STARLIGHT: Formation of the First Stars' under the project number 339177 (RSK, MM), and the Marie Curie Career Integration Grant GALFORMBHS PCIG11-GA-2012-321608, and the H2020-MSCA-RISE-2015 Grant No. StronGrHEP-690904 (EB). RSK acknowledges support from the DFG via SFB 881, 'The Milky Way System' (sub-projects B1, B2 and B8) and from SPP 1573 'Physics of the Interstellar Medium'. VB was supported by NSF grant AST-1413501. AS gratefully acknowledges support through NSF grant AST-1211729 and by NASA grant NNX13AB84G. We thank the GALFORM team to make their code publicly available.

REFERENCES

Abadie J., et al., 2010, Classical and Quantum Gravity, 27, 173001
Abbott B. P., et al., 2009, Advanced LIGO anticipated sensitivity curves, `https://dcc.ligo.org/LIGO-T0900288/public`
Abbott B. P., et al., 2015, LIGO Document G1501223-v3, H1 Calibrated Sensitivity Spectra Oct 1 2015 (Representative for Start of O1), `https://dcc.ligo.org/LIGO-G1501223/public`
Abbott B. P., et al., 2016a, arXiv:1602.03847
Abbott B. P., et al., 2016b, Phys. Rev. Lett., 116, 061102
Abbott B. P., et al., 2016c, arXiv:1602.03842
Ajith P., et al., 2008, Phys. Rev., D77, 104017
Ajith P., et al., 2009, Phys. Rev. D, 79, 129901
Allen B., Romano J. D., 1999, Phys. Rev. D, 59, 102001
Amaro-Seoane P., Santamaría L., 2010, ApJ, 722, 1197
Behroozi P. S., Silk J., 2015, ApJ, 799, 32
Belczynski K., Bulik T., Rudak B., 2004, ApJ, 608, L45
Belczynski K., Buonanno A., Cantiello M., Fryer C. L., Holz D. E., Mandel I., Miller M. C., Walczak M., 2014, ApJ, 789, 120
Belczynski K., Holz D. E., Bulik T., O'Shaughnessy R., 2016, arXiv:1602.04531
Belczynski K., Repetto S., Holz D. E., O'Shaughnessy R., Bulik T., Berti E., Fryer C., Dominik M., 2016, ApJ, 819, 108
Bromm V., 2013, Reports on Progress in Physics, 76, 112901
Clark P. C., Glover S. C. O., Klessen R. S., Bromm V., 2011, ApJ, 727, 110
Cutler C., Flanagan É. E., 1994, Phys. Rev. D, 49, 2658
de Mink S. E., Belczynski K., 2015, ApJ, 814, 58
de Mink S. E., Mandel I., 2016, arXiv:1603.02291
Dominik M., Belczynski K., Fryer C., Holz D. E., Berti E., Bulik T., Mandel I., O'Shaughnessy R., 2012, ApJ, 759, 52
Dominik M., Belczynski K., Fryer C., Holz D. E., Berti E., Bulik T., Mandel I., O'Shaughnessy R., 2013, ApJ, 779, 72
Dominik M., Berti E., O'Shaughnessy R., Mandel I., Belczynski K., Fryer C., Holz D. E., Bulik T., Pannarale F., 2015, ApJ, 806, 263
Dopcke G., Glover S. C. O., Clark P. C., Klessen R. S., 2013, ApJ, 766, 103
Dvorkin I., Vangioni E., Silk J., Uzan J.-P., Olive K. A., 2016, arXiv:1604.04288
Finn L. S., Chernoff D. F., 1993, Phys. Rev. D, 47, 2198
Glover S., 2013, in Wiklind T., Mobasher B., Bromm V., eds, The First Galaxies Vol. 396 of Astrophysics and Space Science Library, The First Stars. p. 103
Graff P. B., Buonanno A., Sathyaprakash B. S., 2015, Phys. Rev. D, 92, 022002
Greif T. H., 2015, Comput. Astrophys. Cosmol., 2, 3
Greif T. H., et al., 2011, ApJ, 737, 75
Haehnelt M. G., 1994, MNRAS, 269, 199
Hartwig T., Bromm V., Klessen R. S., Glover S. C. O., 2015a, MNRAS, 447, 3892
Hartwig T., Latif M. A., Magg M., Bromm V., Klessen R. S., Glover S. C. O., Whalen D. J., Pellegrini E. W., Volonteri M., 2015b, arXiv:1512.01111
Haster C.-J., Wang Z., Berry C. P. L., Stevenson S., Veitch J., Mandel I., 2016, MNRAS, 457, 4499
Heger A., Woosley S. E., 2002, ApJ, 567, 532
Inayoshi K., Kashiyama K., Visbal E., Haiman Z., 2016, arXiv:1603.06921
Johnson J. L., Dalla Vecchia C., Khochfar S., 2013, MNRAS, 428, 1857
Kinugawa T., Inayoshi K., Hotokezaka K., Nakauchi D., Nakamura T., 2014, MNRAS, 442, 2963
Kinugawa T., Miyamoto A., Kanda N., Nakamura T., 2016, MNRAS, 456, 1093
Kroupa P., 1995, MNRAS, 277
Kulczycki K., Bulik T., Belczyński K., Rudak B., 2006, A&A, 459, 1001
Loeb A., 2016, ApJ, 819, L21
Maggiore M., 2007, Gravitational Waves. Vol. 1: Theory and Experiments. Oxford Master Series in Physics, Oxford University Press
Oh S., Kroupa P., Pflamm-Altenburg J., 2015, ApJ, 805,

92
Parkinson H., Cole S., Helly J., 2008, MNRAS, 383, 557
Perna R., Lazzati D., Giacomazzo B., 2016, ApJ, 821, L18
Phinney E. S., 2001, arXiv:0108028
Planck Collaboration 2015, arXiv:1502.01589
Rodriguez C. L., Chatterjee S., Rasio F. A., 2016, arXiv:1602.02444
Rosado P. A., 2011, Phys. Rev. D, 84, 084004
Sana H., et al., 2012, Science, 337, 444
Schneider R., Ferrara A., Ciardi B., Ferrari V., Matarrese S., 2000, MNRAS, 317, 385
Sesana A., 2016, arXiv:1602.06951
Sesana A., Gair J., Mandel I., Vecchio A., 2009, ApJ, 698, L129
Smith R. J., Glover S. C. O., Clark P. C., Greif T., Klessen R. S., 2011, MNRAS, 414, 3633
Stacy A., Bromm V., 2013, MNRAS, 433, 1094
Stacy A., Bromm V., Lee A. T., 2016, arXiv:1603.09475
Thrane E., Romano J. D., 2013, Phys. Rev. D, 88, 124032
Veitch J., Pürrer M., Mandel I., 2015, Physical Review Letters, 115, 141101
Visbal E., Haiman Z., Bryan G. L., 2015, MNRAS, 453, 4456
Woosley S. E., 2016, arXiv:1603.00511

This paper has been typeset from a TEX/ LATEX file prepared by the author.